Monatshefte für Chemie 137, 751–763 (2006)
DOI 10.1007/s00706-006-0473-5

Monatshefte für Chemie
Chemical Monthly
Printed in Austria

Chlorophyll Breakdown in Maize: On the Structure of Two Nonfluorescent Chlorophyll Catabolites[#]

Joachim Berghold[1], **Thomas Müller**[1], **Markus Ulrich**[1], **Stefan Hörtensteiner**[2], and **Bernhard Kräutler**[1,*]

[1] Institute of Organic Chemistry and Center of Molecular Biosciences, Leopold-Franzens-Universität Innsbruck, Innsbruck, Austria
[2] Institute of Plant Sciences, Universität Bern, Bern, Switzerland

Received March 17, 2006; accepted March 21, 2006
Published online May 15, 2006

Summary. In extracts of senescent leaves of the maize plant *Zea mays*, two colorless compounds with UV/Vis-characteristics of nonfluorescent chlorophyll catabolites (NCCs) were detected and tentatively named *Zm*-NCCs. The constitution of the two polar *Zm*-NCCs was determined by spectroscopic means, which confirmed both of these tetrapyrroles to have the basic ligand structure typical of the NCCs from (other) senescent higher plants. In the less polar catabolite, named *Zm*-NCC-2, the core structure was conjugated at the 8^2-position with a glucopyranose unit. *Zm*-NCC-2 had the same constitution as *Nr*-NCC-2, an NCC from tobacco (*Nicotiana rustica*). Indeed, the two NCCs were identified (further) based on their HPL-chromatographic and NMR-spectroscopic properties. The more polar NCC from maize, *Zm*-NCC-1, differed from *Zm*-NCC-2 by carrying a dihydroxyethyl side chain instead of a vinyl group at the 3-position. In earlier work on polar NCCs, only separate glucopyranosyl- and dihydroxyethyl-functionalities were detected. *Zm*-NCC-1 thus is a new constitutional variant of the structures of NCCs from senescent higher plants.

Keywords. Chlorophyll; Chlorophyll catabolism; Mass spectrometry; NMR-spectroscopy; Tetrapyrrole.

Introduction

The seasonal appearance and disappearance of the chlorophylls probably is the most visual sign of life on earth, observable even from outer space [1, 2]. Chlorophyll breakdown also accompanies a variety of pathogenic defects and is a clear symptom of leaf senescence, a form of programmed cell death in plants [3]. It is estimated that more than 10^9 tons of chlorophyll are biosynthesized and degraded

* Corresponding author. E-mail: bernhard.kraeutler@uibk.ac.at
[#] Dedicated to Prof. *Peter Schuster* on the occasion of his 65th birthday

every year on earth [4]. Yet, the riddle of chlorophyll breakdown and the appearance of autumnal colors in the foliage of deciduous trees has remained a remarkable mystery until about fifteen years ago (see *e.g.* Refs. [2–5]). Around 1990 colorless polar compounds were discovered in senescent primary leaves of barley

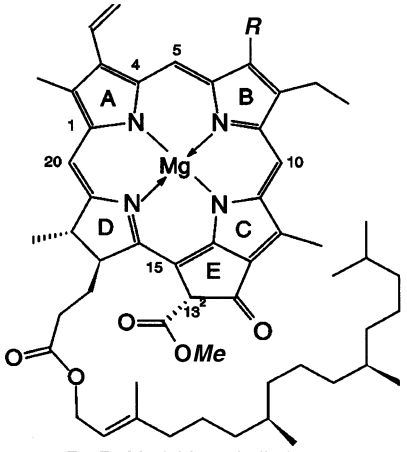

7a *R*=*Me* (chlorophyll a)
7b *R*=HC=O (chlorophyll b)

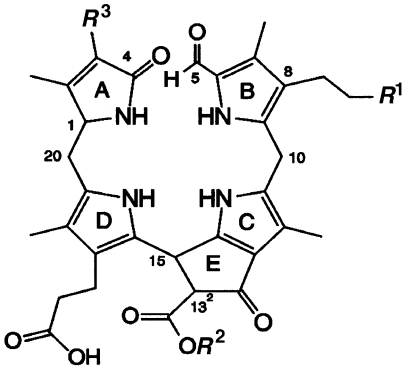

Nonfluorescent chlorophyll catabolities
(NCCs **1-6** and **8** from higher plants)

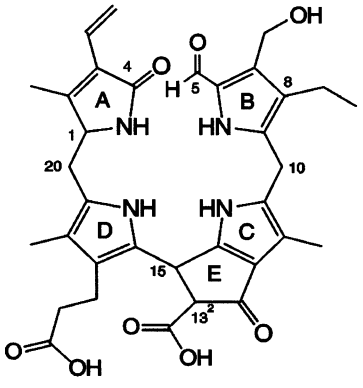

6c *At*-NCC-3

Compound	R^1	R^2	R^3
1 *Hv*-NCC-1	OH	*Me*	$CH(OH)CH_2OH$
2a *Bn*-NCC-1	O-*Mal*	H	$CH=CH_2$
2b *Bn*-NCC-2	O-*β*-*Glc*	H	$CH=CH_2$
2c *Bn*-NCC-3	OH	H	$CH=CH_2$
3a *Cj*-NCC-1	OH	*Me*	$CH=CH_2$
3b *Cj*-NCC-2	H	*Me*	$CH=CH_2$
4a *So*-NCC-1	OH	H	$CH(OH)CH_2OH$
4b *So*-NCC-2	OH	*Me*	$CH(OH)CH_2OH$
4c *So*-NCC-3	OH	H	$CH=CH_2$
4d *So*-NCC-4	OH	*Me*	$CH=CH_2$
4e *So*-NCC-5	H	*Me*	$CH=CH_2$
5a *Nr*-NCC-1	O-*β*-(6′-O-*Mal*)*Glc*	*Me*	$CH=CH_2$
5b *Nr*-NCC-2	O-*β*-*Glc*	*Me*	$CH=CH_2$
6a *At*-NCC-1	O-*β*-*Glc*	H	$CH=CH_2$
6b *At*-NCC-2	OH	H	$CH=CH_2$
6e *At*-NCC-5	H	H	$CH=CH_2$
8a *Zm*-NCC-1	O-*β*-*Glc*	*Me*	$CH(OH)CH_2OH$
8b *Zm*-NCC-2	O-*β*-*Glc*	*Me*	$CH=CH_2$

Abbreviations: *Mal* = malonyl; *Glc* = glucopyranosyl

Fig. 1. Structural formulae of chlorophyll *a* and *b* (**7a**, **7b**) and constitutional formulae of the nonfluorescent chlorophyll catabolites (NCCs): *Hv*-NCC-1 (**1**, from barley, *Hordeum vulgare*) [7], *Bn*-NCCs (**2a**–**2c**, from oilseed rape, *Brassica napus*) [11, 12], *Cj*-NCC-1 (**3a**), *Cj*-NCC-2 (**3b**, from *Cercidiphyllum japonicum*) [14, 15], *So*-NCCs (**4a**–**4e**, from spinach, *Spinacia oleracea*) [16], *Nr*-NCCs (**5a**, **5b**, from tobacco, *Nicotiana rustica*) [17], and *At*-NCCs (**6a**–**6e**, from *Arabidopsis thaliana*) [18, 19]; atom-numbering of the listed NCCs according to IUPAC for the chlorophylls (see *e.g.* Ref. [1])

(*Hordeum vulgare*), which were suggested to be chlorophyll catabolites [6]. The structure of one of them was characterized as the ''nonfluorescent'' chlorophyll catabolite *Hv*-NCC-1 (**1**) [7, 8] (see Fig. 1). It gave the first clues on the major structural transformations responsible for the color changes that occur in chlorophyll breakdown in plants [9, 10].

Over the last fifteen years, about a dozen constitutionally different NCCs from higher plants were detected and analyzed structurally, among them the *Bn*-NCCs **2a**–**2c** from oilseed rape (*Brassica napus*) [11, 12], a common NCC from *Liquidambar styraciflua* [13] and from *Cercidiphyllum japonicum* (called *Cj*-NCC-1, **3a**) [14], as well as a second, less polar NCC from this tree (*Cj*-NCC-2, **3b**) [15], five *So*-NCCs **4a**–**4e** [16] from degreened leaves of spinach (*Spinacia oleracea*), two *Nr*-NCCs **5a** and **5b** from tobacco (*Nicotiana rustica*) [17], and five *At*-NCCs **6a**–**6e** from the model plant *Arabidopsis thaliana* [18, 19] (see Fig. 1). The NCCs are deposited into the vacuoles of senescent leaves [20, 21] and appear to represent the final stages of chlorophyll catabolism in higher plants [9, 10]. However, an urobilinogenoic chlorophyll catabolite was found in isolates obtained from senescent primary leaves of barley, which was suggested to be the result of further oxidative loss of the formyl group of **1** [22].

With the exception of *At*-NCC-3 (**6c**) (from *A. thaliana*) [19] all known nonfluorescent chlorophyll catabolites (NCCs) from senescent plant leaves exhibit the same structural pattern as the NCC **1** and possess a methyl group at the 7-position (just as chlorophyll *a* (**7a**) itself) [9, 10]. Indeed, in the unique catabolite *At*-NCC-3 (**6c**) a hydroxymethyl group is present at this position [19]. NCCs that carry a formyl group at position 7, *i.e.* that would be more closely related to chlorophyll *b* (**7b**), are lacking completely from higher plants (red catabolites derived from **7b** have been found in the green alga *Chlorella protothecoides* [23]). This remarkable pattern of the NCCs in higher plants was explained by the discovery of reductases that reduce chlorophyll(ide) *b* to chlorophyll(ide) *a*, prior to further breakdown [24–26]. The typical nonfluorescent chlorophyll catabolites (NCCs) from senescent higher plants thus exhibit constitutional side chain variability at three positions (3, 8, and 13^2) only [9, 19].

Chlorophyll breakdown in the maize plant *Zea mays* has recently become a subject of special interest: In the course of a search for the ring cleaving enzyme, pheophorbide *a* oxygenase (PaO), two polar fractions in de-greening maize leaves were tentatively suggested to contain NCCs [27]. Pheophorbide *a* oxygenase (PaO) from maize turned out to be identical with the earlier described protein coded by the *lethal leaf spot 1* (*LLS1*, [28]) gene in maize and homologous to that encoded by *accelerated cell death 1* (*ACD1*, [29]) in *Arabidopsis thaliana*. In addition to investigating the structures of NCCs from *A. thaliana* [18, 19], we were thus particularly interested in also identifying the products of chlorophyll breakdown in senescent leaves of *Zea mays*. We report here on the structures of the two polar NCCs found in de-greened maize leaves, *Zm*-NCC-1 (**8a**) and *Zm*-NCC-2 (**8b**).

Results and Discussion

Two polar, colorless, and nonfluorescent chlorophyll catabolites (NCCs) were tentatively identified in extracts of senescent leaves of maize, *Zea mays*, using

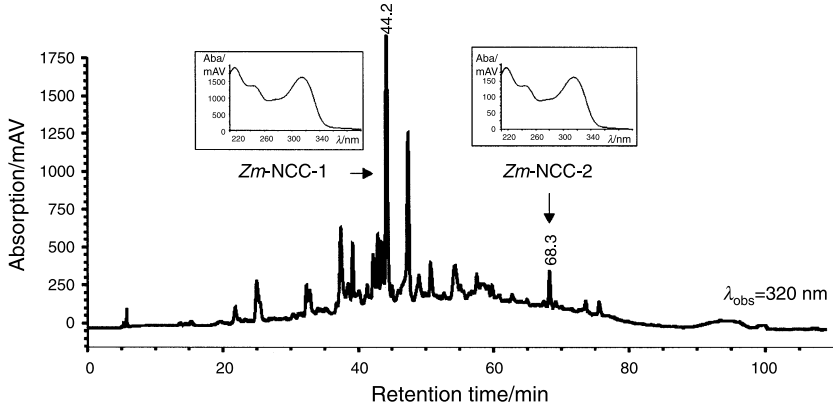

Fig. 2. Analytical HPLC trace (recorded at $\lambda = 320$ nm) of the raw extract of senescent maize leaves, obtained as described in the Experimental; inset: UV/Vis-traces of the fractions containing *Zm*-NCC-1 (**8a**) and *Zm*-NCC-2 (**8b**)

analytical HPLC and based on the characteristic UV-absorbance properties of NCCs [10, 11] (see Fig. 2). Their isolation was achieved, as basically described elsewhere [16]: from 475 g (wet weight) of senescent leaves of *Zea mays* 30 mg (35.7 μmol) of the polar *Zm*-NCC-1 (**8a**) and 5 mg (6.1 μmol) of the less polar *Zm*-NCC-2 (**8b**) were isolated by extraction followed by a two-stage purification procedure based on HPLC. The significantly differing HPLC retention times on a stationary "reversed" phase (*Zm*-NCC-1 (**8a**): 44.2 min, *Zm*-NCC-2 (**8b**): 68 min) reflect the different polarities of **8a** and **8b** (Fig. 2).

The UV/Vis-spectra of the two catabolites, *Zm*-NCC-1 (**8a**) and *Zm*-NCC-2 (**8b**), matched those of **1**, and the longest wavelength maximum in the spectra of **8a** and **8b** was observed at 314 nm. This absorbance is characteristic of an α-formylpyrrole moiety, as present in the NCCs as ring B. The CD spectra of both of the catabolites were similar and matched that of **1** also, suggesting C(15) to have the same configuration as in **1** (and as in all the known natural NCCs from higher plants [9, 15]).

The molecular formula of *Zm*-NCC-2 (**8b**) was determined as $C_{41}H_{50}N_4O_{13}$ by high resolution fast atom bombardment (FAB) mass spectrometry in the (+)-ion mode (reviewed in Ref. [30]), by which method the pseudo-molecular ion $[M + H]^+$ was observed at $m/z = 807.3454 \pm 0.001$. The signals of 41 of the 50 protons were detected in 500 MHz ^{1}H NMR spectra of **8b** in CD_3OD: one singlet (at low field) for the formyl proton, four singlets (at high field) for the four methyl groups attached at the β-pyrrole positions, and one singlet at 3.75 ppm (due to a methyl ester function) were observed. In addition, the typical signal pattern for an unsubstituted peripheral vinyl group was detected in the intermediate field range, near 6 ppm. From ^{1}H,^{13}C-heteronuclear NMR-correlations (such as from HSQC, HMBC, and HSQC-TOCSY spectroscopy [31]) of **8b** in CD_3OD complete assignment of the signals due to ^{1}H- and ^{13}C-nuclei could be achieved (see Table 1). The site of the attachment of the sugar moiety at $H_2C(8^2)$ was indicated (also) by ^{1}H,^{1}H-homonuclear correlations from COSY and ROESY-spectra (see Fig. 3) [31]. The shifts of the ^{1}H and ^{13}C signals for the methylene group $H_2C(8^2)$ were

Table 1. Signal assignment for 500 MHz ^{1}H NMR and 125 MHz ^{13}C NMR spectra of *Zm*-NCC-1 (**8a**) and *Zm*-NCC-2 (**8b**) (at two concentrations) in CD_3OD; ^{13}C assignment of signals from HSQC and HMBC spectra

Assignment	*Zm*-NCC-1 (**8a**) (40 m*M*)		*Zm*-NCC-2 (**8b**) (13 m*M*)		*Zm*-NCC-2 (**8b**) (0.35 m*M*)
	$\delta(^{1}H)$/ppm	$\delta(^{13}C)$/ppm	$\delta(^{1}H)$/ppm	$\delta(^{13}C)$/ppm	$\delta(^{1}H)$/ppm
C(1)	4.04	62.4	4.01	61.8	4.01
C(2)		158.8		156.6	
C(2^{1})	2.04	12.4	1.98	12.3	1.98
C(3)		131.4			
C(3^{1})	4.56	68.4	6.45	127.5	6.45
C(3^{2})	3.63, 3.69	65.7	5.35, 6.10	119.4	5.35, 6.10
C(4)		175.0		174.5	
C(5)	9.32		9.29		9.29
C(6)		129.0		128.9	
C(7)		135.4		135.3	
C(7^{1})	2.24	8.6	2.22	8.7	2.23
C(8)		120.5		120.6	
C(8^{1})	2.66	25.0	2.64	25.0	2.64
C(8^{2})	3.38, 3.75	70.3	3.40, 3.74	70.3	3.41, 3.74
C(9)		139.3		139.4	
C(10)	3.98, 4.04	23.8	3.96, 4.06	23.8	3.96, 4.05
C(11)		134.1		133.9	
C(12)		112.2		112.4	
C(12^{1})	2.09	9.1	2.12	9.2	2.12
C(13)		125.8		125.8	
C(13^{2})		67.7		67.7	
C(13^{3})		171.6		171.6	
C(13^{5})	3.75	52.6	3.75	52.6	3.75
C(14)		161.2		161.5	
C(15)	4.89	37.1	4.89	37.1	4.89
C(16)		124.3		124.5	
C(17)		120.3		120.5	
C(17^{1})	2.62, 2.72	21.8	2.64, 2.74	22.0	2.64, 2.72
C(17^{2})	2.31	39.2	2.32	39.4	2.32
C(17^{3})		181.0		181.2	
C(18)		115.2		115.3	
C(18^{1})	1.92	9.2	1.92	9.1	1.92
C(19)		124.3		124.6	
C(20)	2.50, 2.89	29.5	2.40, 2.88	30.3	2.43, 2.88
C(1′)	4.19	104.6	4.18	104.6	4.18
C(2′)	3.17	75.0	3.17	75.1	3.17
C(3′)	3.37	77.8	3.38	77.8	3.38
C(4′)	3.26	71.2	3.26	71.3	3.26
C(5′)	3.26	77.6	3.26	77.7	3.26
C(6′)	3.66, 3.83	62.4	3.64, 3.84	62.5	3.64, 3.84

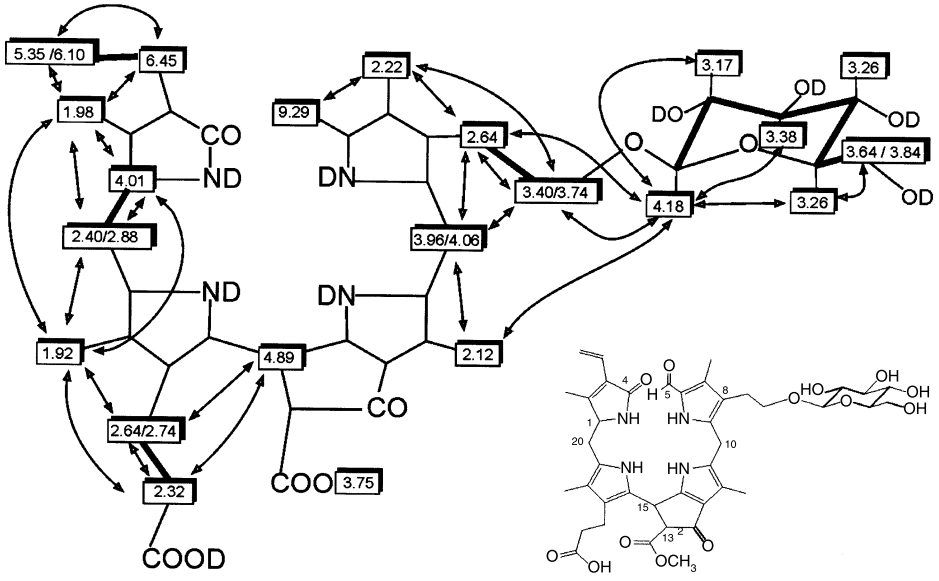

Fig. 3. Graphical representations of the ^{1}H NMR chemical shift values of *Zm*-NCC-2 (**8b**) and of their homonuclear correlations in CD_3OD; signal assignments of carbon-bound hydrogen atoms (solid arrows represent ROESY correlations; bold lines indicate TOCSY correlations (see Ref. [31])

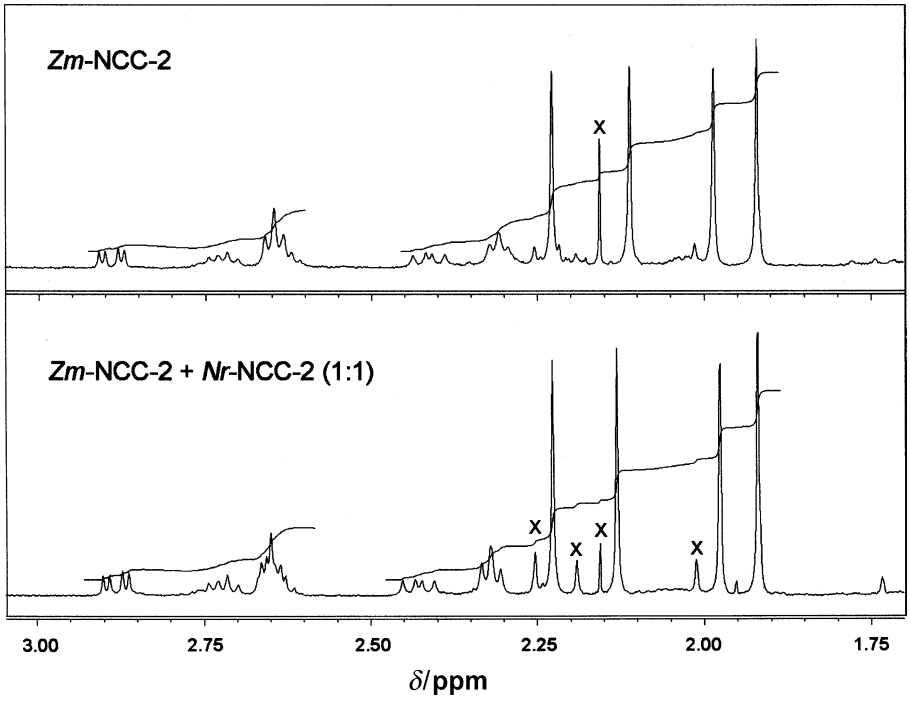

Fig. 4. Identification of *Zm*-NCC-2 (**8b**) and of *Nr*-NCC-2 (**5b**) [17] by comparison of 500 MHz ^{1}H NMR spectra: high field section of the spectrum of *Zm*-NCC-2 (**8b**, 0.35 m*M*) and of a (1:1) mixture of *Zm*-NCC-2 (**8b**) and of *Nr*-NCC-2 (**5b**, 0.35 m*M*) (additional signals, marked by an X, are likely to be due to the 13^2-epimer or are solvent impurities)

consistent with an oxygen bridge to the peripheral sugar substituent. The latter was identified as a β-glucopyranoside unit by comparing the ^{1}H and ^{13}C shifts with the spectra of methyl-β-*D*-glucopyranoside [32], as well as by comparing the NMR-spectra of **8b** with those of *Bn*-NCC-2 (**2b**) and *Nr*-NCC-2 (**5b**), where a peripheral β-glucopyranosyl group at C(8^2) was found earlier [11, 17]. Indeed, the NCCs **5b** and **8b**, not only turned out to have the same constitution, but they were identified (with each other) by HPL-chromatographic and ^{1}H NMR-spectroscopic analysis: the latter was made unambiguous, by actually recording the ^{1}H NMR spectrum of **8b**, as well as of a 1:1 mixture of the two NCCs **5b** and **8b**. The latter spectrum displayed a single and exactly matching set of (the relevant) signals (see Fig. 4). Such a means of identification was used, as the ^{1}H NMR spectra of solutions of *Zm*-NCC-2 (**8b**) (and *e.g.* of *Nr*-NCC-2 (**5b**)) in deuteromethanol suffered from an apparent lack of precise reproducibility of ^{1}H chemical shift values. This observation is in line with earlier findings [15], which suggested a strong susceptibility of some signal positions to slightly differing solution compositions.

The molecular formula of *Zm*-NCC-1 (**8a**) was determined as $C_{41}H_{52}N_4O_{15}$ from the signal position of the pseudo-molecular ion $[M+H]^+$, which was observed at $m/z = 841.356 \pm 0.005$ in a high resolution fast atom bombardment (FAB) mass spectrum in the (+)-ion mode. In the spectra of both **8a** and **8b** a signal of $m/z = 684.3$ was observed, indicating the characteristic loss of ring A from the pseudo-molecular ion $[M+H]^+$ (corresponding to a loss of 157 mass units in the spectrum of **8a** or of 123 mass units in the spectrum of **8b**). This fragmentation pattern is characteristic of the FAB-mass spectra of the NCCs [9, 16]. In addition, a prominent signal at $m/z = 775.4$ in the spectrum of **8b** indicated the loss of 32 mass units, as detected similarly in the spectra of other NCCs due to fragmentation of the methyl ester functionality at C(13^2) [16]. The signals of 41 of the 52 hydrogens of **8a** were detected in the 500 MHz ^{1}H NMR spectrum of **8a** in CD_3OD: one singlet (at low field) for the formyl proton, four singlets (at high field) for the four methyl groups attached at the β-pyrrole positions, and one singlet at 3.75 ppm (due to a methyl ester function) were observed. However, in contrast to the ^{1}H NMR spectrum of **8b**, the signals typical for a peripheral vinyl group were absent. Instead, ^{1}H,^{13}C-heteronuclear NMR-correlations (HSQC, HMBC, and HSQC-TOCSY spectroscopy [31]) allowed the detection in the spectrum of **8a** in CD_3OD of the signals due to a 1,2-dihydroxyethyl side chain, and complete assignment of the signals due to ^{1}H and ^{13}C nuclei could be also achieved once more (see Fig. 5 and Table 1). The sugar moieties of **8a** and **8b**, identified as a β-glucopyranoside group bound at C(8^2), gave rise to a virtually super-imposable set of signals in the spectra of both *Zm*-NCCs. The site of attachment for the peripheral glucopyranosyl substituent at C(8^2) and the bridging oxygen O(8^3), primarily indicated from ROESY-spectra, were consistent also with the typical downfield shifts of the ^{1}H and ^{13}C signals of $H_2C(8^2)$.

The spectroscopic data thus indicate the tetrapyrrolic cores of the two *Zm*-NCCs **8a** and **8b** to have a common build-up, including a common relative stereochemistry at the chiral centers C(1), C(13^2), and C(15): The CD-spectra of **8a** and **8b** are consistent with the configuration of C(15) in the *Zm*-NCCs to be the same as that found, so far, in all of the natural NCCs from higher plants [9, 10]. This chiral center is indicated to arise from a nonenzymatic, stereoselective isomerization of

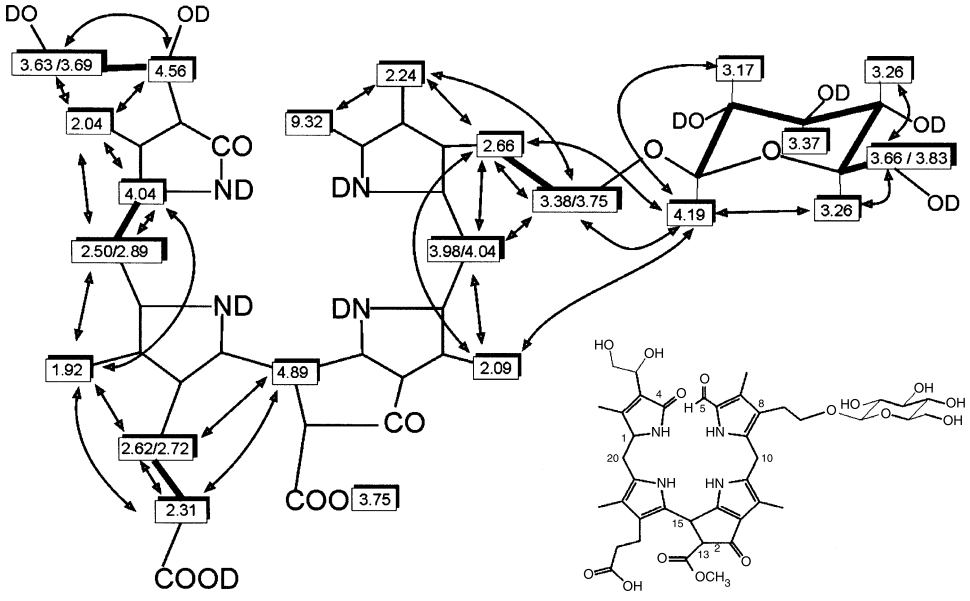

Fig. 5. Graphical representations of the ^{1}H NMR chemical shift values of *Zm*-NCC-1 (**8a**) and of their homonuclear correlations in CD_3OD; signal assignments of carbon-bound hydrogen atoms (solid arrows represent ROESY correlations; bold lines indicate TOCSY correlations (see Ref. [31])

fluorescent chlorophyll catabolite (FCC) precursors [33, 34] to the corresponding NCCs [15]. The relative configuration at C(15) and C(13^2), with HC(15) suggested *cis* to the methoxycarbonyl group at C(13^2) in (the prevailing epimer of) **8a** and **8b** is likely result of a nonenzymatic equilibration reaction at the acidic β-ketoester position C(13^2), which adjusts its configuration to that at C(15). The latter process would occur in the vacuoles of senescent plant cells [15], but it may also take place while the isolated NCCs are kept in a protic solution.

The available NMR data show the peripheral functionalization at C(8^2) of the *Zm*-NCCs to make use of the same β-glucopyranosyl moiety, as in *Bn*-NCC-2 (**2b**) from oilseed rape (*Brassica napus*) and in *Nr*-NCC-2 (**5b**) from tobacco. The further structural and analytical data suggest the (common) configuration of the *Zm*-NCCs **8a** and **8b** at C(1) to be the same as in the glucosylated *Nr*-NCCs **5a** and **5b**, and (therefore) to be opposite to that in *Bn*-NCC-2 (**2b**).

The NCCs (and the FCCs) fall into two classes with respect to the configuration at C(1) due to the evolution of two types of RCC-reductases (RCCR) in higher plants, which provide the primary fluorescent chlorophyll catabolites (pFCCs) [33–36]. It is thus of interest to note the mutual relationships for the *Zm*-NCCs with respect to their type of peripheral refunctionalization and their stereochemistry at C(1). Analysis of the type of pFCC produced in *Zea mays* was achieved by the use of a standard coupled oxygenase/reductase assay [36], employing the reductase from *Zea mays*. It suggested the primary FCC from maize to be the same as the FCC in *Capsicum annuum* (sweet pepper), *i.e.* to be the 1-*epi*-pFCC [34], and differing from the one in oilseed rape (*Brassica napus*) (see Fig. 6) [33, 36]. The two *Zm*-NCCs, **8a** and **8b**, would thus be deduced to belong to the "C(1)-*epi*"-series also, consistent with the identity of the *Zm*-NCC-2 (**8b**) and *Nr*-NCC-2 (**5b**).

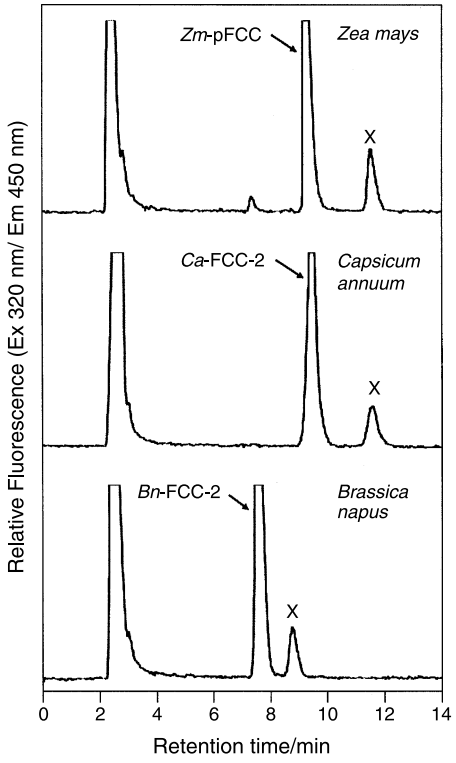

Fig. 6. Analysis of the stereoselectivity of the reductase (RCCR) from maize and other plant species based on the standard oxygenase/RCC-reductase assay [36] and HPLC with fluorescence detection at 450 nm to monitor the FCCs formed; traces obtained with RCCR from maize (*Zea mays*: 1-*epi*-pFCC, top), from sweet pepper (*Capsicum annuum*: 1-*epi*-pFCC = *Ca*-FCC-2 [34], middle), and canola (*Brassica napus*: pFCC = *Bn*-FCC-2 [33], bottom); the signals due to the FCCs are highlighted (additional signals, marked by an X, are likely to be due to the corresponding 13^2-epimers)

The indicated availability of two related NCCs (**8a** and **8b**) from a single plant (maize) parallels the occurrence of NCCs with a range of peripheral groups, observed in other senescent plants [9, 16, 18]. Our finding on the *Zm*-NCCs provides further support for the view that, the main constitutional variations of the chlorophyll catabolites in various higher plants concern enzyme catalyzed, peripheral refunctionalization reactions. The peripheral adaptations with polar functions have been suggested to be of relevance for the transport and the final deposition of chlorophyll catabolites in the vacuoles [5, 20, 21, 37].

Conclusion

In the present work, the structures of *Zm*-NCC-1 (**8a**) and *Zm*-NCC-2 (**8b**) have been characterized, two nonfluorescent chlorophyll catabolites (NCCs) from senescent leaves of the maize plant *Zea mays*. Fortunately, the constitutions of NCCs can be delineated with little ambiguity by modern spectroscopic means, from the NMR-derived connectivity, in particular [2, 9, 10]. Some progress also has been made towards establishing the pattern of the relative stereochemistry at the chiral centers of the reduced tetrapyrrolic skeleton, *e.g.* by means of structural correlations of the

NCCs from various plant sources (see *e.g.* Ref. [38]). Whereas the basic build-up of **8a** and **8b** is the same as known for all NCCs from higher plants, the more polar *Zm*-NCC-1 (**8a**) exhibits a previously unknown constitution. The identification of the *Zm*-NCCs thus provides further evidence, first of all, for the occurrence of a variety of catabolic transformations in chlorophyll breakdown in higher plants. It also underlines the relevance of extensive peripheral refunctionalization in the course of chlorophyll breakdown under natural growth conditions. Our accumulated findings point to the occurrence of at least six basic types of peripheral catabolic transformations in the later phases of chlorophyll breakdown, some of which operate (sequentially or even parallel, see Fig. 1) in a particular senescent plant. These transformations involve only four sites for the known peripheral functionalities. While the earlier phases of chlorophyll breakdown in higher plants are likely to pass through a remarkably stringent entry point, the mono-oxygenation of pheophorbide *a* [27, 39] (but see Ref. [19]), the rather diverse structures of the NCCs, as displayed in senescent leaves of maize and in other plants, may be taken to indicate the later phases to follow less consistently evolved and (possibly) also less strictly regulated pathways.

Experimental

General

Reagents used were reagent-grade from Sigma-Aldrich and Fluka. HPLC solvents were from Merck (Darmstadt, Germany). Sep-Pak-C18-cartridges were from Waters Associates and Sephadex G25 fine from Amersham Biotech. Analytical HPLC: Column: Hypersil ODS 5 μm, 250×4.6 mm id, 0.5 cm^3/min (A: *Me*OH, B: 0.1 *M* potassium phosphate, *pH* = 7.0, 0–10 min 20% A/80% B; 10–70 min: Linear gradient to 60% A/40% B. Preparative HPLC: Column: Hypersil ODS 5 μm, 250×21.2 mm id, 5 cm3/min (A: *Me*OH, B: potassium phosphate buffer, *pH* 7.0) HPLC: HP 1100 (diode array detector), solvents were degassed by a vacuum degasser. All chromatograms were taken at rt and data was processed by HP Chemstation for 3D. UV/Vis-Spectra: Hitachi-U3000 spectrophotometer. CD Spectra: Jasco-J715 spectropolarimeter. NMR Spectra: Varian Unity$_{plus}$ 500 $\delta(HOD) = 4.76$ ppm, $\delta(C^1HD_2OD) = 3.31$ ppm and $\delta(^{13}CD_3OD) = 49.0$ ppm [32]. MS: Finnigan MAT 95-S positive-ion mode; FAB-MS [30]: cesium gun, 20 keV, matrix: glycerin.

Isolation of Zm-NCCs

475 g senescent, freshly harvested *Zea mays* leaves were cut into small pieces and mixed for 10 min with 2600 cm^3 *Me*OH/100 m*M* potassium phosphate (*pH* = 8.0) 1/1 (*v*/*v*) using a 600 W hand blender. The suspension was filtered through a dish towel and the solid residue was mixed again with 1000 cm^3 *Me*OH/0.1 *M* potassium phosphate (*pH* = 8.0) 1/1 (*v*/*v*). After filtration the combined filtrates were diluted 1:1 with methanol, chilled down to 4°C for 15 min and centrifuged for 3 min at 6000 rpm. The pooled supernatants were concentrated to 2000 cm^3 at rt in *vacuo*. After diluting with 1000 cm^3 water the solution was applied to a Sep-Pak-C18 cartridge (Waters) in two portions. The eluent was collected for further purifications of *Zm*-NCC-1 (**8a**, see below).

Isolation of Zm-NCC-2 (**8b**, *3^1,3^2-didehydro-8^2-(1-β-glucopyranosyl)-oxy-1,4,5,10,15,20,22,24-(21H,23H)-octahydro-13^2-(methoxycarbonyl)-4,5-dioxo-4,5-seco-phytoporphyrinate*, $C_{41}H_{50}N_4O_{13}$)

The cartridge was washed twice with 10 cm^3 water, and crude **8b** was eluted with 10 cm^3 *Me*OH. After evaporation of the solvent under high vacuum, the solid residue was redissolved and applied to preparative HPLC using a linear gradient from 53% A to 61% A in 30 min. The fractions containing

8b were pooled, desalted on a Sep-Pak cartridge, and dried under high vacuum. Two more runs of preparative HPLC (the *pH* of the potassium phosphate buffer in the third run was changed from 7.0 to 6.6) followed by Sep-Pak desalting (see above) were performed to obtain 5 mg *Zm*-NCC-2 (**8b**).

Isolation of Zm-NCC-1 (**8a**, *3^1,3^2-dihydroxy-8^2-(1-β-glucopyranosyl)-oxy-1,4,5,10,15,20,22,24-(21H,23H)-octahydro-13^2-(methoxycarbonyl)-4,5-dioxo-4,5-seco-phytoporphyrinate*, $C_{41}H_{52}N_4O_{15}$)

The raw eluate containing **8a** was extracted twice using petrol ether (bp 40–60°C) and the aqueous phase was concentrated under high vacuum near room temperature. The residual aqueous solution was then applied in four portions to a Sep-Pak-C18 cartridge (Waters). The cartridge was washed twice with 10 cm^3 water, and crude **8a** was eluted with 10 cm^3 *Me*OH. After evaporation of the solvents under high vacuum, solid raw **8a** was purified by preparative HPLC using the step gradient 5 min at 20% A and 25 min at 37% A. The fractions containing **8a** were pooled, desalted on a Sep-Pak cartridge, and dried under high vacuum. Raw **8a** was purified further by two more runs of preparative HPLC (a solvent mixture with 39% A was used in the third run) followed by desalting with Sep-Pak cartridges (see above) to obtain 32 mg *Zm*-NCC-1 (**8a**).

Selected spectroscopic data of Zm-NCC-1 (**8a**)

UV/Vis (*Me*OH, $c = 4.26 \times 10^{-5}$ *M*): λ (logε) = 242 (4.26), 314 (4.26) nm; CD (*Me*OH, $c = 4.26 \times 10^{-5}$ *M*): λ ($\Delta\varepsilon$) = 225 (18.2), 252 (−5.4), 282 (−13.3), 315 (3.4) nm; ^{1}H NMR (500 MHz, 26°C, 40 m*M* in CD_3OD): $\delta = 1.92$ (s, $H_3C(18^1)$), 2.04 (s, $H_3C(2^1)$), 2.09 (s, $H_3C(12^1)$), 2.24 (s, $H_3C(7^1)$), 2.31 (m, $H_2C(17^2)$), 2.50 (dd, $J = 8.6$, 14.6 Hz, $H_AC(20)$), 2.67 (m, 4H, $H_2C(8^1)$ and $H_2C(17^1)$), 2.89 (dd, $J = 4.4$, 13.9 Hz, $H_BC(20)$), 3.17 (dd, $J = 8.1$, 9.5 Hz, HC(2′)), 3.26 (m, 2H, HC(4′) and HC(5′)), 3.38 (m, 2H, $H_AC(8^2)$ and HC(3′)), 3.66 (m, 3H, $H_AC(3^2)$, $H_BC(3^2)$, and $H_AC(6')$), 3.75 (m, $H_BC(8^2)$ superimposed by 3.75 (s, 3H, $H_3C(13^5)$), 3.83 (d, $J = 11.0$, $H_BC(6')$), 4.04 (m, 3H, $H_2C(10)$ and HC(1)), 4.19 (d, $J = 8.1$ Hz, HC(1′)), 4.56 (dd, $J = 5.1$, 6.6 Hz, $HC(3^1)$), 4.89 (s, HC(15)), 9.32 (s, HC(5)) ppm; ^{13}C NMR (125 MHz, 26°C, 40 m*M* in CD_3OD, data from HSQC and HMBC [31]): see Table 1; FAB-MS: m/z (%) = 863.4 (14, $M + Na^+$), 843.4 (23), 842.4 (54), 841.4 (100, $M + H^+$), 684.3 (34, M-Ring A + H^+); HR-FAB-MS: found 841.35560 ($[M + H]^+$ calcd 841.3507).

Selected spectroscopic data of Zm-NCC-2 (**8b**)

UV/Vis (*Me*OH, $c = 4.28 \times 10^{-4}$ *M*): λ (logε) = 242 (4.28), 314 (4.22) nm; CD (*Me*OH, $c = 4.26 \times 10^{-4}$ *M*): λ ($\Delta\varepsilon$) = 225 (18.2), 258 (−5.6), 282 (13.3), 315 (3.4) nm; ^{1}H NMR (500 MHz, 26°C, 13 m*M* in CD_3OD): $\delta = 1.92$ (s, $H_3C(18^1)$), 1.98 (s, $H_3C(2^1)$), 2.12 (s, $H_3C(12^1)$), 2.22 (s, $H_3C(7^1)$), 2.32 (m, $H_2C(17^2)$), 2.40 (dd, $J = 9.5$, 14.4 Hz, $H_AC(20)$), 2.64 (m, 3H, $H_AC(17^1)$ and $H_2C(8^1)$), 2.74 (m, $H_BC(17^1)$), 2.88 (dd, $J = 4.6$, 14.4 Hz, $H_BC(20)$), 3.17 (dd, $J = 8.0$, 9.0 Hz, HC(2′)), 3.26 (d, broad, 2H, HC(4′) and HC(5′)), 3.39 (m, 2H, $H_AC(8^2)$ and HC(3′)), 3.64 (dd, $J = 4.6$, 12.0 Hz, $H_AC(6')$), 3.75 (s, $H_3C(13^5)$), 3.74 (m, $J = 7.8$ Hz, $H_BC(8^2)$) superimposed by 3.84 (d, $J = 12.0$ Hz, $H_BC(6')$), 3.99 (m, 3H, $H_2C(10)$ and HC(1)), 4.18 (d, $J = 7.8$ Hz, HC(1′)), 4.89 (s, HC(15)), 5.35 (dd, $J = 2.0$, 11.7 Hz, $H_AC(3^2)$), 6.10 (dd, $J = 2.2$, 17.6 Hz, $H_BC(3^2)$), 6.45 (dd, $J = 11.7$, 17.8 Hz, $HC(3^1)$), 9.29 (s, HC(5)) ppm; ^{1}H NMR (500 MHz, 26°C, 2 m*M* in D_2O): $\delta = 1.85$ (s, $H_3C(18^1)$), 1.89 (s, $H_3C(2^1)$), 2.08 (s, $H_3C(12^1)$), 2.15 (s, $H_3C(7^1)$), 2.18 (m, $H_AC(17^2)$), 2.27 (m, $H_AC(17^2)$), 2.60 (m, $H_2C(17^1)$), 2.66 (m, 3H, $H_AC(20)$ and $H_2C(8^1)$), 2.82 (dd, $J = 3.9$, 14.7 Hz, $H_BC(20)$), 3.22 (t, $J = 8.8$ Hz, HC(2′)), 3.35 (m, 2H, HC(4′) and HC(5′)), 3.42 (m, HC(3′)), 3.48 (m, $H_AC(8^2)$), 3.67 (dd, $J = 4.8$, 12.7 Hz, $H_BC(8^2)$), 3.74 (m, $H_AC(6')$), 3.79 (s, $H_3C(13^5)$), 3.85 (d, $J = 11.7$ Hz, $H_BC(6')$), 3.93 (m, 3H, $H_2C(10)$ and HC(1)), 4.30 (d, $J = 7.8$ Hz, HC(1′)), 4.87 (s, HC(15)), 5.40 (d, $J = 11.7$ Hz, $H_AC(3^2)$), 5.83 (d, $J = 18.6$ Hz, $H_BC(3^2)$), 6.35 (dd, $J = 11.7$, 17.6 Hz, $HC(3^1)$), 9.08 (s, HC(5)) ppm; ^{13}C NMR (125 MHz, 26°C, 13 m*M* in CD_3OD, data from HSQC and HMBC [31]): see Table 1; FAB-MS: m/z (%) = 845.3 (17, $M + K^+$), 829.3 (40, $M + Na^+$), 809.4 (30), 808.4 (57), 807.4 (100, $M + H^+$), 775.4 (11, M–MeOH + H^+), 693.3 (21), 684.3 (42, M-Ring A + H^+); HR-FAB-MS: found 807.34543 ($[M + H]^+$, calcd 807.3447).

Coupled Oxygenase/RCC-reductase assays

Extracts from leaves (maize, canola) or fruits (pepper) containing the soluble proteins, including the respective RCC-reductases (RCCR), were prepared and the proteins were precipitated with ammonium sulfate (80% saturation), as described [36]. After desalting on Sephadex G50, the RCCR-containing extracts [36] were employed in standard coupled oxygenase/reductase assays [37, 40], as follows: Assays (total volume of 50 mm^3) contained partially purified oxygenase from canola, equivalent to 0.5 g of tissue [39], RCCR (equivalent to 50 mg of tissue) and 0.5 m*M* pheophorbide *a* [37] as substrate. They were supplemented with cofactors as described [18] and incubated at room temperature for 1 h in the dark. After the addition of 80 mm^3 of methanol, formation of pFCCs was monitored with a fluorescence detector (320/450 nm) after reversed-phase HPLC separation with 36% (*v*/*v*) 50 m*M* potassium phosphate buffer *pH* 7.0 in methanol as solvent.

Acknowledgements

We would like to thank *S. Berger* for practical assistance, *S. Gschösser* and *K.-H. Ongania* for providing NMR spectroscopic and mass spectrometric data. Financial support by the Austrian National Science Foundation (Project No. P-16097) and the Swiss National Science Foundation (Project No. 3100A0-105389) is also gratefully acknowledged.

References

[1] Scheer H (ed) Chlorophylls (1991) CRC-Press, Boca Raton, USA
[2] Kräutler B, Matile P (1999) Acc Chem Res **32**: 35
[3] Buchanan BB, Gruissem W, Jones RL (eds) Biochemistry and Molecular Biology of Plants (2001) Am Soc Plant Physiologists, Rockville, USA
[4] Brown SB, Houghton JD, Hendry GAF (1991) Chlorophyll breakdown. In: Scheer H (ed) Chlorophylls, CRC Press, Boca Raton, USA, p 465
[5] Matile P, Hörtensteiner S, Thomas H, Kräutler B (1996) Plant Physiol **112**: 1403
[6] Bortlik KH, Peisker C, Matile P (1990) J Plant Physiol **136**: 161
[7] Kräutler B, Jaun B, Bortlik KH, Schellenberg M, Matile P (1991) Angew Chem Int Ed **30**: 1315
[8] Kräutler B, Jaun B, Amrein W, Bortlik KH, Schellenberg M, Matile P (1992) Plant Physiol Biochem **30**: 333
[9] Kräutler B (2003) Chlorophyll breakdown and chlorophyll catabolites. In: Kadish KM, Smith KM, Guilard R (eds) The Porphyrin Handbook, vol 13, Elsevier Science, Amsterdam, p 183
[10] Kräutler B, Hörtensteiner S (2006) Chlorophyll Catabolites and the Biochemistry of Chlorophyll Breakdown. In: Grimm B, Porra R, Rüdiger W, Scheer H (eds) Chlorophylls and Bacteriochlorophylls: Biochemistry, Biophysics, Functions and Applications, vol 25. Advances in Photosynthesis and Respiration, Springer, Dordrecht, The Netherlands, p 237
[11] Mühlecker W, Kräutler B, Ginsburg S, Matile P (1993) Helv Chim Acta **76**: 2976
[12] Mühlecker W, Kräutler B (1996) Plant Physiol Biochem **34**: 61
[13] Iturraspe J, Moyano N, Frydman B (1995) J Org Chem **60**: 6664
[14] Curty C, Engel N (1996) Phytochemistry **42**: 1531
[15] Oberhuber M, Berghold J, Breuker K, Hörtensteiner S, Kräutler B (2003) Proc Natl Acad Sci USA **100**: 6910
[16] Berghold J, Breuker K, Oberhuber M, Hörtensteiner S, Kräutler B (2002) Photosynth Res **74**: 109
[17] Berghold J, Eichmüller C, Hörtensteiner S, Kräutler B (2004) Chemistry & Biodiversity **1**: 657
[18] Pružinska A, Tanner G, Aubry S, Anders I, Haldimann P, Moser S, Müller T, Ongania KH, Kräutler B, Youn J-Y, Liljegren SJ, Hörtensteiner S (2005) Plant Physiol **139**: 52
[19] Müller T, Moser S, Ongania KH, Hörtensteiner S, Kräutler B (2006) Chem Bio Chem **7**: 40
[20] Matile P, Ginsburg S, Schellenberg M, Thomas H (1988) Proc Natl Acad Sci USA **85**: 9529

[21] Hinder B, Schellenberg M, Rodoni S, Ginsburg S, Vogt E, Martinoia E, Matile P, Hörtensteiner S (1996) J Biol Chem **271**: 27233
[22] Losey FG, Engel N (2001) J Biol Chem **276**: 8643
[23] Engel N, Curty C, Gossauer A (1996) Plant Physiol Biochem **34**: 77
[24] Ito H, Ohysuka T, Tanaka A (1996) J Biol Chem **271**: 1475
[25] Scheumann V, Schoch S, Rüdiger W (1999) Planta **209**: 364
[26] Rüdiger W (2003) The last step of chlorophyll synthesis. In: Kadish KM, Smith KM, Guilard R (eds) The Porphyrin Handbook, vol 13, Elsevier Science, Amsterdam, p 71
[27] Pružinská A, Tanner G, Anders I, Roca M, Hörtensteiner S (2003) Proc Natl Acad Sci USA **100**: 15259
[28] Gray J, Close PS, Briggs SP, Johal GS (1997) Cell **89**: 25
[29] Greenberg JT, Ausubel F (1993) Plant J **4**: 327
[30] Watson TR (1995) Fast atom bombardment. In: Matsuo T, Caprioli RM, Gross ML, Seyama Y (eds) Biological mass spectrometry present and future, John Wiley & Sons, Chichester, p 24
[31] Kessler H, Gehrke M, Griesinger C (1988) Angew Chem Int Ed **2**: 490
[32] Pretsch E, Bühlmann P, Affolter C (2000) Structure determination of organic compounds, Springer Verlag, Berlin
[33] Mühlecker W, Ongania KH, Kräutler B, Matile P, Hörtensteiner S (1997) Angew Chem Int Ed **36**: 401
[34] Mühlecker W, Kräutler B, Moser D, Matile P, Hörtensteiner S (2000) Helv Chim Acta **83**: 278
[35] Wüthrich KL, Bovet L, Hunziker PE, Donnison IS, Hörtensteiner S (2000) Plant J **21**: 189
[36] Hörtensteiner S, Rodoni S, Schellenberg M, Vicentini F, Nandi OI, Qiu YL, Matile P (2000) Plant Biol **2**: 63
[37] Hörtensteiner S, Vicentini F, Matile P (1995) New Phytol **129**: 237
[38] Oberhuber M, Berghold J, Mühlecker W, Hörtensteiner S, Kräutler B (2001) Helv Chim Acta **84**: 2615
[39] Hörtensteiner S, Wüthrich KL, Matile P, Ongania KH, Kräutler B (1998) J Biol Chem **273**: 15335
[40] Rodini S, Mühlecker W, Kräutler B, Moser D, Thomas H, Matile P, Hörtensteiner S (1997) Plant Physiol **115**: 669